Theor Chem Acc (2010) 127:475–484
DOI 10.1007/s00214-010-0735-5

REGULAR ARTICLE

A theoretical investigation on the spectroscopic properties and photosensitizing capability of 5, 10, 15, 20-tetraphenylsapphyrin and 5, 10, 15, 20-tetraphenyl-26,28-diheterosapphyrins with two O, S, or Se Atoms

Ramón López · M. Isabel Menéndez · Mireya Santander-Nelli · Gloria I. Cárdenas-Jirón

Received: 9 November 2009 / Accepted: 6 February 2010 / Published online: 21 February 2010

Abstract A density functional theory (DFT) study of the V/UV spectrum and the adiabatic energy released from the triplet excited state of sapphyrin and three disubstituted derivatives (with O, S or Se atoms) is performed in order to obtain an accurate theoretical description of their capability as photosensitizers in photodynamic therapy (PDT). For the calculation of the V/UV spectra, we used two functionals already tested for porphyrin derivatives, B3LYP and PBE0, and two new ones recently proposed, MPWB1 K and M05, all of them with two different basis sets and two continuum solvent models. The best agreement with experimental data was obtained at the CPCM-M05/6-31 + G(d)//B3LYP/6-31 + G(d) level, at which errors lie in the range of 0.13–0.20 eV for the Q band in CH_2Cl_2 solution. A careful comparison between triplet and singlet geometries shows that the inner macrocycle enlarges, but planarity distortions lead to a volume contraction upon excitation to the triplet state for sapphyrin, and O and S heterosapphyrins, and to negligible volume changes for Se heterosapphyrin. Actually, the heterosapphyrins with S and Se atoms acquire a saddle shape in the triplet state. According to our results, the energy released from the triplet state for S- and Se- disubstituted sapphyrins could be adequate to generate activated oxygen both in the gas phase and in CH_2Cl_2 solution.

Keywords Sapphyrin · Heterosapphyrins · Photosensitizers · TD-DFT · V/UV spectra · Excited states

Electronic supplementary material The online version of this article (doi:10.1007/s00214-010-0735-5) contains supplementary material, which is available to authorized users.

R. López · M. I. Menéndez (✉)
Departamento de Química Física y Analítica,
Facultad de Química, Universidad de Oviedo,
C/Julián Clavería 8, 33006 Oviedo, Asturias, Spain
e-mail: isabel@uniovi.es

M. Santander-Nelli · G. I. Cárdenas-Jirón (✉)
Laboratorio de Química Teórica,
Departamento de Ciencias del Ambiente,
Facultad de Química y Biología,
Universidad de Santiago de Chile (USACH),
Casilla 40, Correo 33, Santiago, CHILE
e-mail: gloria.cardenas@usach.cl

1 Introduction

Sapphyrins are expanded porphyrin derivatives whose core contains an additional pyrrole ring giving rise to a bipyrrole subunit (see Scheme 1). They present potential medical use in several areas and have been considered as potential photodynamic therapy agents in the treatment of cancer diseases [1, 2]. Sapphyrins are important in coordination chemistry and have been proposed as anion transporters [3–5], among other practical applications [6]. They constitute a growing family of compounds, which have been the subject of many investigations in these years [3, 4, 7–11].

Recently, a variety of modified sapphyrins have been prepared. Among them, are the heterosapphyrins in which some core NH groups belonging to a pyrrole have been replaced by other donor atoms such as O, S, and Se. The incorporation of these heteroatoms into the core of the macrocycle leads to an alteration of the cavity size and electronic structure, thus providing interesting spectroscopic, chemical, and physical properties, which can find applications in biology, medicine, material science, and catalysis [12]. 5,10,15,20-Tetraphenylheterosapphyrins have been synthesised in the 1990s [13–17], and several surprising facts concerning their conformation have been reported. ^{1}H NMR spectroscopic studies suggest that

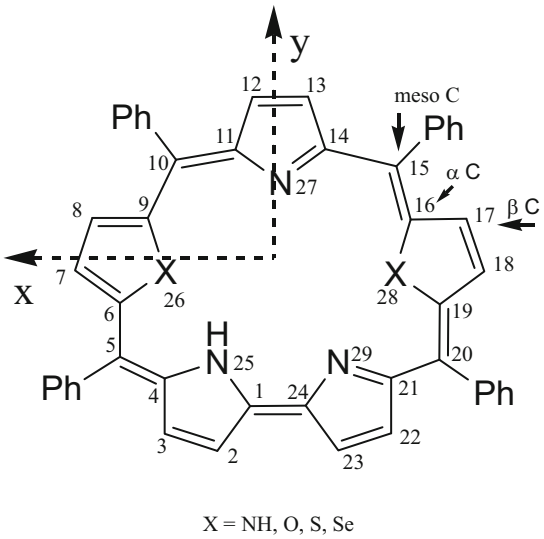

Scheme 1 Atom numbering in sapphyrins

5,10,15,20-tetraphenylsapphyrin and 5,10,15,20-tetraphenyl-dioxasapphyrin present the pyrrole ring opposite the bipyrrolic unit inverted (*inverted* conformation) while diheterosapphyrins with S and Se show the three N atoms toward the internal cavity (*normal* conformation) [13, 16]. On the other hand, DFT calculations on sapphyrin and dioxasapphyrin without meso substituents render the *normal* conformation as the most stable one [18, 19].

In a previous work, we undertook a theoretical analysis of 5,10,15,20-tetraphenylsapphyrin, **TPS,** 5,10,15,20-tetraphenyl-26,28-dioxasapphyrin, **TP2OS**, 5,10,15,20-tetraphenyl-26,28-dithiasapphyrin, **TP2SS,** and 5,10,15,20-tetraphenyl-26,28-diselenasapphyrin, **TP2SeS**, and proposed several reasons for the greater stability of the inverted conformation of **TPS** and **TP2OS** (**i-TPS, i-TP2OS**), and the normal conformation of **TP2SS** and **TP2SeS** (**n-TP2SS** and **n-TP2SeS**) [20]. In that work and in the present one, the most stable tautomer of each sapphyrin is considered. **TPS** tautomer with H atoms bonded to N25, N27, and N28 is the selected one. For the heterosapphyrins, the degenerate tautomers with internal H atom bound to N25 or N29 atoms are reported to be the most stable ones [18] so tautomer N25 will be studied.

The feature we wish to remark in this study is the theoretical description of the ability of just mentioned sapphyrins as photosensitizers that could be used in photodynamical therapy (PDT) for the treatment of cancer and other diseases [8–10]. PDT uses a photosensitizer, working as a light-sensitive drug, to treat the target tissue locally upon the irradiation of light with appropriate wavelengths. The mechanism of PDT is based on the interaction between the excited photosensitizer and surrounding molecules, generating singlet oxygen ($^1O_2$), which can cause oxidative damage to biological substrates and ultimately cell death [1]. At experimental level, much work has been performed looking for the best photosensitizers [1, 2, 6, 12–15, 17–19, 21]. One of the criteria that have to be fulfilled is the capability of the photosensitizer to absorb radiation in the therapeutic window, that is, between 600 nm and 850 nm [22, 23]. Light in this spectral region is scattered to a relatively small extent by most mammalian tissues and is poorly absorbed by endogenous chromophores such as melanin, cytochromes, and hemoglobin. As a consequence, this red light possesses a high penetration power into human tissues and can be selectively absorbed by photosensitizing agents localized in predetermined sites of the organism [1].

On the basis of experimental results, the electronic absorption spectra in dichloromethane solution of the sapphyrins **i-TPS, i-TP2OS, n-TP2SS**, and **n-TP2SeS** are composed of two main absorption bands: one at higher wavelengths, in the visible region, called the Q band, and the other, at lower wavelengths and more intense, called the B or Soret band [14–16, 21]. All of them are collected in Table 1, along with their intensities, when available.

The Q band presents four absorption maxima. Theoretical interpretations of the absorption spectra of related systems such as free-base porphins have assigned the four absorption maxima of this band to Q_x^0, Q_x^1, Q_y^0, and Q_y^1, where the subscripts denote the excitation direction and the superscripts the vibration band [24]. The B band displays a split absorption maximum for **i-TPS, i-TP2OS**, and **n-TP2SeS**, and one appreciable absorption maximum at 469 nm for **n-TP2SS**.

As mentioned above, the human body's therapeutic window for PDT falls into the range 600–850 nm [22, 23], being less harmful the longest wavelength radiations. It has been reported that the presence of the heteroatoms O and S in porphyrin derivatives results in a bathochromic effect, that is, a displacement of the absorption wavelength to larger values [25]. This effect is observed in the Q_x^0 and Q_x^1 peaks experimentally measured for the sapphyrins investigated in this work (see Table 1). In the present research, we focus our attention on the displacement of the longest wavelength of the Q band, λ_Q, for the most stable isomers of sapphyrin, **i-TPS,** and the heterosapphyrins **i-TP2OS, n-TP2SS**, and **n-TP2SeS** by performing TD-DFT calculations.

The absorption wavelength criterion itself is not enough; it is also necessary that the photosensitizer has a good quantum yield for the first excited triplet state, which has to release the appropriate energy to yield singlet oxygen, that is, 0.95 eV (22.0 kcal/mol) or greater [12]. This value is the minimum energy necessary to excite the triplet ground state of the molecular oxygen ($^3O_2$) to its first excited singlet state ($^1O_2$) of lower energy named as $^1\Delta_g$. The next excited singlet state of the molecular oxygen corresponds

Table 1 Experimental electronic absorption spectra of **i-TPS**, **i-TP2OS**, **n-TP2SS,** and **n-TP2SeS** sapphyrins

	i-TPS [21]		**i-TP2OS** [16]		**n-TP2SS** [14–16]		**n-TP2SeS** [14, 15]	
Q band								
Q_x^0	1.57 (790)	–	1.48 (837)	3.52	1.51 (821)	4.30	1.51 (823)	4.55
Q_x^1	1.75 (710)	–	1.69 (735)	3.44	1.69 (732)	3.67	1.68 (736)	3.85
Q_y^0	1.78 (697)	–	1.97 (630)	3.74	1.99 (624)	4.00	1.96 (631)	4.26
Q_y^1	1.94 (640)	–	2.12 (586)	3.84	2.12 (584)	4.30	2.09 (592)	4.45
Soret band	2.39 (518)	–	2.62 (474)	4.55	2.64 (469)	5.44	2.40 (517)	4.81
	2.51 (493)	–	3.08 (403)	sh			2.61 (475)	5.48

For each band energy (eV), (wavelength (nm)) and log(ε) are shown

to the state $^1\Sigma_g^+$ with excitation energy of 1.63 eV (37.5 kcal/mol). Although both $^1\Delta_g$ and $^1\Sigma_g^+$ are significant in the gas phase, only the $^1\Delta_g$ state is important in condensed phase.

The aim of getting an accurate theoretical description of the photosensitizing properties of these sapphyrins prompted us to undertake a DFT study of the V/UV absorption spectra and of the energy emission from the triplet states of the most stable conformers of **i-TPS**, **i-TP2OS**, **n-TP2SS**, and **n-TP2SeS**, taking into account the effect of the density functional, the basis set, and solvent on these properties.

2 Computational details

Computational investigations of the electronic absorption spectra of regular porphyrins (and several derivatives) have included calculations ranging from semiempirical [26, 27], single and multireference (MR) configuration interaction (CI) [24, 28–35], multiconfiguration second-order perturbation theory (CASPT2) [36–39], and time-dependent density functional theory (TD-DFT) [24, 32, 33, 35, 40, 41]. Excitation energies have also been calculated at the similarity transformed equation-of-motion coupled cluster and perturbation theoretical levels (STEOM-CC and STEOM-PT) [31–42]. The less expensive TD-DFT has been shown to be in better agreement with experiment than the more expensive ab initio CI, CASPT2, or STEOM-CC calculations [24, 28]. Therefore, we calculated the absorption spectra as vertical excitations from the minima of the ground state structures using the TD-DFT [43, 44] framework as implemented in Gaussian03 [45]. The corresponding optimized geometries of the ground-state structures were reported in a previous theoretical study [20]. They were found using the B3LYP functional [46–48], with the relativistic effective core pseudopotential LACVP for Se [49], and the 6-31 + G(d) [50] basis set for the remaining atoms as implemented in the JAGUAR program [51].

Given that the absorption spectra of some porphyrin derivatives, calculated by using the B3LYP/6-31G(d) [52, 53] and PBE0/6-31 + G(d) [22, 23] levels of theory, are in good agreement with experimental results, we used several computational schemes by combining the functionals B3LYP and PBE0 [54, 55] with the basis sets 6-31 + G(d) (LANL2DZ for Se) [49] and 6-311 + G(d,p) [50] (LANL2DZ for Se). The hybrid functional B3LYP is based on Becke's three parameter hybrid exchange functional and gradient-corrected correlation functional of Lee et al. while PBE0 consists of the generalized gradient functional PBE (Perdew-Burke-Erzenrhof) with 25% of Hartree–Fock exchange energy. Besides these functionals, which were already tested in the literature, we also performed TD-DFT calculations with MPWB1 K [56, 57] and M05 [58, 59] functionals recently developed. The experimental absorption spectra of porphyrin derivatives are known to be solvent dependent, and in order to account for this dependency, we carried out calculations using two continuum models: a dielectric-like polarizable continuum model (PCM) [60–62] and a conductor-like polarizable continuum model (C-PCM) [63–66]. A dielectric constant of 8.93 was assumed in the calculations to simulate dichloromethane as the solvent experimentally used.

Full geometry optimizations of the triplet state structures of all the investigated sapphyrins were performed at the UB3LYP/6-31 + G(d) (LACVP for Se) theory level as implemented in the JAGUAR program. Similar computational schemes (B3LYP/6-31G(d) [52, 53] and PBE0/6-31 + G(d) [22, 23]) have been previously employed to determine the geometry and energy of the triplet-state structures of different porphyrin systems. Molecular volumes were defined as the volume inside a contour of 0.001 electrons/bohr^3, and calculated with Gaussian03 [45]. The effect of CH_2Cl_2 solvent on the triplet–singlet electronic energy gap was also calculated by means of self-consistent reaction field Poisson–Boltzmann (SCRF-PB) [62] model. Finally, the electronic structure of the triplet species studied in this work was investigated using the natural bond orbital (NBO) approach [67].

3 Results and discussion

3.1 Electronic absorption spectra

Table 2 collects the excitation energies and oscillator strengths of λ_Q theoretically obtained for **i-TPS, i-TP2OS, n-TP2SS,** and **n-TP2SeS** molecules. As they are the largest wavelengths computationally obtained, we compare them to the longest (and most intense) λ_Q value experimentally measured, on the basis of previous theoretical works on related systems [24].

Let's analyze first the results obtained with density functionals already tested for porphyrin derivatives. For the four sapphyrins optimized at the B3LYP/6-31 + G(d) theory level and with the eight computational levels used, PCM-B3LYP/6-31 + G(d), PCM-B3LYP/6-311 + G(d,p), PCM-PBE0/6-31 + G(d), PCM-PBE0/6-311 + G(d,p), CPCM-B3LYP/6-31 + G(d), CPCM-B3LYP/6-311 + G(d,p), CPCM-PBE0/6-31 + G(d), CPCM-PBE0/6-311 + G(d,p); the calculated Q wavelength, λ_Q, is smaller than the experimental one as observed in previous similar theoretical works [22]. The enlargement of the basis set from 6-31 + G(d) to 6-311 + G(d,p) makes λ_Q longer by 2 or 3 nm, so it is changed in the right direction. The effect, however, is very small compared to the increase in the required computational effort, so we chose 6-31 + G(d) basis set as a practical one. Based on reported results and as a first step, we tested B3LYP and PBE0 functionals. Table 2 shows that PBE0 renders λ_Q values smaller than B3LYP ones by about 9 or 10 nm, so B3LYP is a better functional for the calculation of the Q band for this family of sapphyrins. The last variable considered in the selection of the best computational scheme is the continuum model used to simulate bulk solvent effects. We found that PCM and CPCM yield essentially the same results with an increase in λ_Q values of about 1 nm when using CPCM. So, among the eight computational approaches tested by now, we select CPCM-B3LYP/6-31 + G(d) as the most adequate one. The energy differences between the results obtained at this level and the experimental ones are 0.16, 0.21, 0.20, and 0.19 eV for **i-TPS, i-TP2OS, n-TP2SS,** and **n-TP2SeS**, respectively.

Among the new density functionals which have been recently developed to offer a broad applicability in chemistry [56, 68–70], we choose MPWB1 K and M05 to test their ability to theoretically reproduce spectroscopic measurements. Taking into account previous discussion to select an appropriate basis set and solvent model, we carried out TD-DFT calculations at the CPCM-MPWB1 K/6-31 + G(d) (LANL2DZ for Se) and CPCM-M05/6-31 + G(d) (LANL2DZ for Se) levels of theory on the B3LYP/6-31 + G(d) (LACVP for Se) optimized geometries. Again, both functionals yield shorter λ_Q values than experimental ones, rendering MPWB1 K functional worse results than those obtained at the previously selected level CPCM-B3LYP/6-31 + G(d). On the other hand, M05 yields λ_Q values closer to experimental ones, so CPCM-M05/6-31 + G(d)//B3LYP/6-31 + G(d) is the best computational level to reproduce λ_Q values among those tested by us, and the energy differences between the results obtained at this level and experimental ones are 0.13, 0.20, 0.17, and 0.15 eV for **i-TPS, i-TP2OS, n-TP2SS,** and **n-TP2SeS**, respectively. These errors are lower than other theoretical ones reported for different porphyrin derivatives [22, 23].

All previous TD-DFT calculations have been carried out using B3LYP/6-31 + G(d) (LACVP pseudopotential for Se) optimized structures. To check whether this theory level for the geometry optimization could bias our results, we performed geometry optimizations with the M05 functional (See Online Resource 1) and, then, TD-DFT calculations with both B3LYP and M05 functionals (See Table 2). As discussed above, using B3LYP geometries, the functional M05 renders λ_Q values closest to experiment (See bold rows 1 and 2 in Table 2). The same conclusion rises when M05 optimized structures are used to perform the B3LYP and M05 TD-DFT calculations (See bold rows 3 and 4 in Table 2). It seems that M05 is an adequate functional to calculate electronic spectra for the systems considered in this work. On the other side, the comparison of λ_Q values obtained with B3LYP TD-DFT calculations over B3LYP and M05 geometries (See bold rows 1 and 3 in Table 2) indicates that B3LYP geometries are the most suitable. The same conclusion is obtained when λ_Q values are calculated through M05 TD-DFT calculations (See bold rows 2 and 4 in Table 2). Therefore, B3LYP geometries yield electronic spectra more similar to experimental ones. In fact, although B3LYP and M05 optimized geometries are quite similar, the bond distances along the inner macrocycle of **n-TP2SS** and **n-TP2SeS** at the M05/6-31 + G(d) optimized geometries differ from X ray data in the range of −0.099 Å to +0.031 Å, while the same bond distances are closer to experimental values in B3LYP/6-31 + G(d) optimized structures (differences between −0.014 Å and +0.038 Å) (No X-Ray data are available for **i-TPS** and **i-TP2OS**) [20]. As a consequence, the combination of B3LYP optimized geometries with M05 TD-DFT calculations provides the best values of λ_Q for the systems under study.

In good agreement with experimental measurements, our calculations show that heterosubstitution by two O, S, and Se at 26 and 28 positions in the sapphyrin molecule causes a red shift of the longest λ_Q value relative to the unsubstituted sapphyrin.

Table 2 Calculated excitation energies in eV (in parenthesis in nm) and oscillator strengths at different levels of theory, and comparison with experimental data for the Q band of 5,10,15,20-tetraphenylsapphyrin and 5,10,15,20-tetraphenyl-26,28-diheterosapphyrins with two O, S, and Se atoms in CH_2Cl_2 solution

	i-TPS		**i-TP2OS**		**n-TP2SS**		**n-TP2SeS**	
	Excitat. energy eV (nm)	Oscillator strength	Excitat. energy eV (nm)	Oscillator strength	Excitat. energy eV (nm)	Oscillator strength	Excitat. energy eV (nm)	Oscillator strength
Experiment	1.57 (790)		1.48 (837)	3.52[a]	1.51 (821)	4.30[a]	1.51 (823)	4.55[a]
PCM-B3LYP/6-31 + G(d)// B3LYP/6-31 + G(d)	1.74 (714)	0.110	1.69 (731)	0.164	1.72 (722)	0.163	1.70 (727)	0.163
PCM-B3LYP/6-311 + G(d,p)// B3LYP/6-31 + G(d)	1.73 (717)	0.103	1.69 (733)	0.157	1.71 (724)	0.156	1.70 (730)	0.155
PCM-PBE0/6-31 + G(d)// B3LYP/6-31 + G(d)	1.76 (703)	0.119	1.72 (720)	0.171	1.74 (713)	0.171	1.73 (718)	0.170
PCM-PBE0/6-311 + G(d,p)// B3LYP/6-31 + G(d)	1.76 (705)	0.111	1.72 (722)	0.163	1.73 (715)	0.163	1.72 (721)	0.162
***1*-CPCM-B3LYP/6-31 + G(d)// B3LYP/6-31 + G(d)**	**1.73 (715)**	**0.123**	**1.69 (733)**	**0.179**	**1.71 (723)**	**0.177**	**1.70 (729)**	**0.177**
CPCM-B3LYP/6-311 + G(d,p)// B3LYP/6-31 + G(d)	1.73 (718)	0.116	1.69 (735)	0.171	1.71 (726)	0.170	1.70 (731)	0.169
CPCM-PBE0/6-31 + G(d)// B3LYP/6-31 + G(d)	1.76 (704)	0.133	1.72 (722)	0.186	1.73 (715)	0.185	1.72 (720)	0.184
CPCM-PBE0/6-311 + G(d,p)// B3LYP/6-31 + G(d)	1.76 (706)	0.124	1.71 (723)	0.178	1.73 (717)	0.176	1.72 (723)	0.175
CPCM-MPWB1 K/6-31 + G(d)// B3LYP/6-31 + G(d)	1.75 (707)	0.131	1.73 (718)	0.182	1.71 (724)	0.185	1.69 (732)	0.186
***2*-CPCM-M05/6-31 + G(d)// B3LYP/6-31 + G(d)**	**1.70 (728)**	**0.138**	**1.68 (739)**	**0.172**	**1.69 (736)**	**0.181**	**1.66 (746)**	**0.180**
***3*-CPCM-B3LYP/6-31 + G(d)// M05/6-31 + G(d)**	**1.75 (707)**	**0.124**	**1.71 (724)**	**0.192**	**1.75 (709)**	**0.179**	**1.74 (711)**	**0.176**
***4*-CPCM-M05/6-31 + G(d)// M05/6-31 + G(d)**	**1.73 (717)**	**0.139**	**1.71 (727)**	**0.188**	**1.72 (721)**	**0.186**	**1.71 (727)**	**0.187**

[a] Experimental log(ε) values

3.2 Molecular orbitals involved in the Q band

The spectroscopic behavior of sapphyrins can be rationalized in terms of the Gouterman four-orbital model [71–74], because the principal excitations involve the two highest occupied molecular orbitals (HOMO and HOMO–1) and the two lowest unoccupied molecular orbitals (LUMO and LUMO + 1). Online Resource 2 collects the contribution of electronic transitions to the Q band. At CPCM-M05/6-31 + G(d)//B3LYP/6-31 + G(d) (LANL2DZ for Se) level, the HOMO → LUMO transition (0-0) is the most important one in all of the sapphyrins, and its weight increases as the atomic number of the heteroatom grows. The second contribution corresponds to the crossed transition HOMO → LUMO + 1 (0-1) for **i-TPS** and **i-TP2OS** and to the HOMO-1 → LUMO + 1 (1-1) transition for **n-TP2SS** and **n-TP2SeS**.

Figure 1 displays the shape of these MOs for the four sapphyrins under study in this work. Unoccupied MOs LUMO, and LUMO + 1, and the occupied HOMO-1 are quite similar for the four sapphyrins, but the HOMO of **i-TPS** shows several differences when compared with the HOMOs of the remaining heterosapphyrins. Pyrrole ring opposite to the bipyrrolic unit displays large contribution of the β carbon atoms only in **i-TPS**. Concerning heterosubstituted rings, they display large participation of the β carbon atoms in the heterosapphyrins but not in **i-TPS**.

In Online Resources 3 and 4, the full electronic spectra for the four sapphyrins at the CPCM-B3LYP/6-31 + G(d)//B3LYP/6-31 + G(d) and CPCM-M05/6-31 + G(d)//B3LYP/6-31 + G(d) levels are collected. These results show that the 3rd and 4th theoretical bands present significantly larger oscillator strengths, so they can be assigned to the Soret band. Only two peaks of the Q band

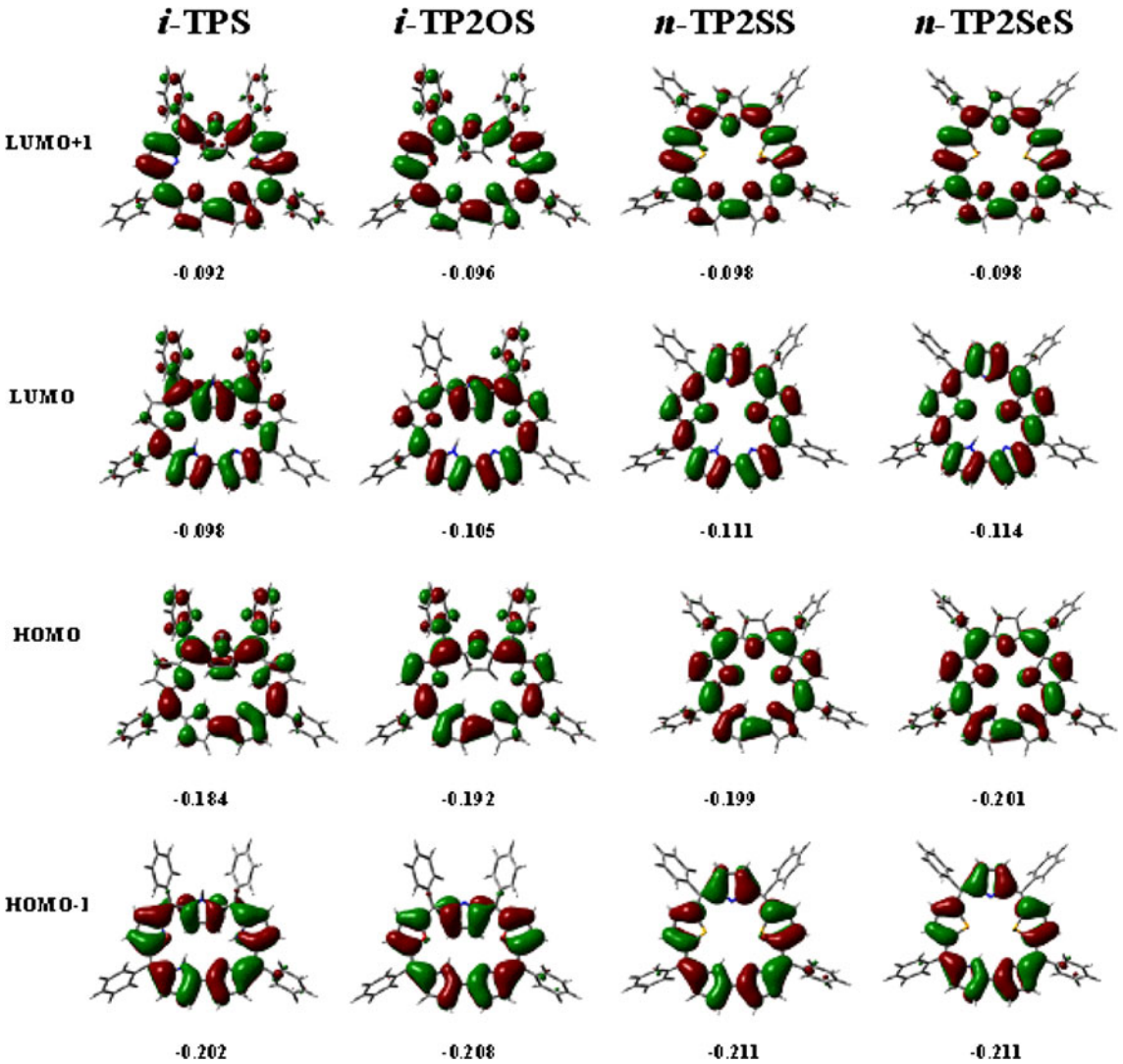

Fig. 1 Frontier MOs of the sapphyrins under study involved in the electronic excitation spectra along with their orbital energies (eV)

are theoretically found, as reported in similar theoretical works on other porphyrin derivatives [22, 23]. As can be seen in Table 1, one of the peaks belonging to the Q_x/Q_y type is more intense than the other. TD-DFT calculations seem to reproduce with significant oscillator strength only the most intense band of each group. In many porphyrin systems, the main configuration of Q_x bands is a combination of HOMO → LUMO, (0-0), and HOMO-1 → LUMO + 1, (1-1) transitions while Q_y band is mainly composed of crossed transitions, (0-1) and (1-0) [22, 23]. Our results indicate that the 1st Q peak theoretically calculated could be clearly assigned to one of the Q_x experimental bands for **n-TP2SS**, and **n-TP2SeS** at the CPCM-M05/6-31 + G(d) level while **i-TPS** and **i-TP2OS** longest λ_Q peak present the contribution of direct and crossed transitions.

3.3 Singlet-state versus triplet-state geometries and energies

Another important goal of our work was to determine the optimized triplet-state structures and energies of **i-TPS, i-TP2OS, n-TP2SS,** and **n-TP2SeS** in order to investigate their emission properties. Online Resource 5 and Table 3 collect the optimized triplet-state structures and their corresponding energy at UB3LYP/6-31 + G(d) (LACVP for Se) theory level, respectively.

We analyzed the geometry of the triplet structures by comparison with the analogous singlet ground state ones taking as reference the atom numbering in sapphyrins shown in Scheme 1. Our results indicate that, when passing from the ground state to the triplet one, the most significant changes in the bond distances correspond to an enlargement of the skeleton comprised between the α carbon atoms C9 and C16 going through N27. It amounts to 0.057, 0.053, 0.045, and 0.037 Å for **i-TPS**, **i-TP2OS**, **n-TP2SS,** and **n-TP2SeS**, respectively. It is also observed an elongation of the internal macrocycle between C6 and C19 going through the bipyrrolic N atoms. In this case, the enlargement is of 0.030, 0.056, 0.067, and 0.057 Å for **i-TPS**, **i-TP2OS**, **n-TP2SS,** and **n-TP2SeS**, respectively. Another significant variation was found for the distance between X26 and X28 (X = N, O, S, Se), which shortens 0.028 Å for **i-TPS** and enlarges 0.005, 0.087, and 0.089 Å for **i-TP2OS**, **n-TP2SS,** and **n-TP2SeS**, respectively. The bond angles involved in the core of the sapphyrins are very similar and present a very slight variation in the range of (−1.2) − (+1.4) degrees when passing from the singlet state to triplet one. More notable changes were found for the dihedral angles, which are directly related to the planarity of the molecules. In the inverted sapphyrins **i-TPS** and **i-TP2OS,** the four rings with their heteroatom oriented toward the inner part of the macrocycle are nearly in the same plane both in the singlet and in the triplet states. In **i-TPS,** the inverted pyrrole ring goes away from this plane by 34.2° in the triplet state, 10.3° more than in the singlet one, as measured by the C9-C10-C11-C12 dihedral angle. However, the opposite is found for **i-TP2OS** in which the inverted ring is 8.3° closer to the reference plane in the triplet state. These reverse deviations could be related to the increase of steric repulsions among core H atoms in **i-TPS** due to the small shortening of the X26-X28 distance, which is only slightly elongated in **i-TP2OS.** Heterosapphyrins in normal conformation, **n-TP2SS** and **n-TP2SeS**, show a significant loss of planarity in the triplet state compared to the singlet one adopting a saddle shape. This fact is observed in the z coordinates of the β carbon atoms (see axis orientation in Scheme 1) that change in the substituted rings with X26 and X28 heteroatoms from a mean value of 0.35 and 0.27 Å to 0.65 and 0.47 Å for **n-TP2SS** and **n-TP2SeS,** respectively, while the pyrrole ring and the bipyrrolic unit vary from −0.38 and −0.29 Å to −0.77 and −0.52 Å for **n-TP2SS** and **n-TP2SeS,** respectively (see Online Resource 6). The slight enlargement of the internal cavity along with the separation of X26 and X28 for X = S, Se upon excitation to the triple state could render weaker interactions inside the macrocycle, that is, an increase in flexibility. As discussed in our pervious work [20], the response of the sapphyrins to the repulsion of *meso* phenyl rings is their bending, when possible.

RMSD (root mean square deviation) allows a general overview of the deviations of the whole molecular structure of the triplet state compared to the singlet one. Between the inverted sapphyrins, **i-TP2OS** (RMSD = 0.43) presents a

Table 3 Total (in hartree) and relative energies (ΔE, in eV) of the most stable isomers of **i-TPS** and 5,10,15,20-tetraphenyl-26,28-diheterosapphyrins with two O, S, and Se atoms in the gas phase and in CH_2Cl_2 solution

Molecule	Electronic state	Gas phase		CH_2Cl_2 solution	
		Total energy	ΔE	Total energy	ΔE
***i*-TPS**					
	^{1}A	−2122.782705	0.0	−2122.798841	0.0
	^{3}A	−2122.750779	0.87	−2122.777099	0.59
***i*-TP2OS**					
	^{1}A	−2162.472980	0.0	−2162.497790	0.0
	^{3}A	−2162.436504	0.99	−2162.465657	0.87
***n*-TP2SS**					
	^{1}A	−2808.425178	0.0	−2808.451806	0.0
	^{3}A	−2808.387111	1.04	−2808.414514	1.01
***n*-TP2SeS**					
	^{1}A	−2030.439868	0.0	−2030.461463	0.0
	^{3}A	−2030.400559	1.07	−2030.426175	0.96

larger structural change than **i-TPS** (RMSD = 0.19), whereas for the normal ones, **n-TP2SS** shows a higher value of RMSD (0.61) than **n-TP2SeS** (0.32), indicating that the compound with sulfur undergoes a major structural change.

It has been reported that laser-induced optoacoustic spectroscopy measures predict a contraction of porphyrin ring in aqueous solution after excitation to the triplet state [75], which mainly originates in the rearrangement of water around the excited macrocycle nitrogen atoms and to a minor extent in bonds shortening upon excitation. In spite of the larger inner cavity theoretically obtained for the triplet state in the sapphyrins under study, the whole volume calculated in the gas phase also displays a reduction for **i-TPS** (-29.7 cm^3/mol), **i-TP2OS** (-23.1 cm^3/mol), and **n-TP2SS** (-39.1 cm^3/mol) and a negligible expansion for **n-TP2SeS** ($+4.5$ cm^3/mol) upon excitation to this excited state.

NBO calculations show that both in singlet and in triplet states, N and O atoms present a negative charge of about -0.5 electrons, while the less electronegative S and Se atoms present a positive charge of about $+0.6$ electrons. Consequently, C_α atoms bonded to negatively charged atoms display a positive charge (about $+0.2$ electrons) and those bonded to positively charge atoms display a negative charge (about -0.2 electrons). In all the cases, C_β atoms in all of the rings have negative charges of about -0.2 electrons. At both electronic states in **i-TPS**, it is observed an important stabilizing interaction (see Online Resource 7) between the lone pair on the N atom of the pyrrole NHs and the two closest meso π antibonding C–C bonds whereas in **i-TP2OS**, **n-TP2SS** and **n-TP2SeS**, the stabilizing interaction of the heteroatom lone pairs with the neighboring π antibonding C–C bonds is much weaker as a consequence of a poorer overlap. This indicates that the O, S, and Se lone pairs in the heterosapphyrins present a lower mobility compared with that of the N lone pairs of the pyrrole NHs in **i-TPS**. Concerning the spin density in the triplet states of the studied sapphyrins, our results show that it is preferentially located on the *meso* carbon atoms C5 and C15. In **i-TPS**, it is also located in the *meso* carbon C10. The inclusion of CH_2Cl_2 as a solvent in the calculations hardly influences NBO atomic charges, stabilizing interactions involving lone pairs of the heteroatoms, and spin densities.

As can be seen in Table 3, in CH_2Cl_2 solution, only the heterosapphyrins with S and Se atoms have an energy gap between the singlet ground and the triplet excited states greater or equal than 0.95 eV, which fulfills the second requirement for their use as photosensitizers in PDT. In the gas phase, it is interesting to note that the increase of the size of the heteroatom X provokes a rise of the energy gap from 0.87 to 1.07 eV. Solvent makes the energy gap smaller for all the sapphyrins as it stabilizes both states but the triplet one in a greater amount.

Our DFT calculations indicate that the S and Se disubstituted sapphyrins fulfill the two requirements to act as good photosensitizers in CH_2Cl_2: they absorb light in the red region and release adequate energy to activate oxygen. However, the solvent used, CH_2Cl_2, is not appropriate to be directly used in physiological conditions. To make our results more applied we could think, on the one hand, about doing again the study for water soluble sapphyrins. This way has already been explored by relevant research groups [76, 77]. On the other hand, it has been recently reported the use of photon upconverting nanoparticles (PUNPs) to design a new generation of versatile photosensitizers [78]. These particles are coated with a layer of silica containing photosensitizing molecules and attached to ill cells via specific antigen–antibody binding. In this nonpolar environment and selecting adequate PUNPs (those emitting the energy that sapphyrins absorb), the sapphyrin and the three heterosapphyrins here studied could be used.

4 Conclusions

In this work, it was found that M05, a recently defined DFT functional, is adequate to theoretically reproduce V/UV spectra of sapphyrin, **i-TPS**, and the heterosapphyrins **i-TP2OS**, **n-TP2SS**, and **n-TP2SeS** in their most stable conformations. CPCM-M05/6-31 + G(d)//B3LYP/6-31 + G(d) seems to be a balanced computational level leading to errors in the Q band in CH_2Cl_2 solution for the just mentioned sapphyrins in the range of 0.13–0.20 eV. The comparison between singlet ground and triplet excited geometries shows a slight enlargement of the inner macrocycle, but changes in planarity lead to small volume contractions upon excitation for **i-TPS**, **i-TP2OS**, and **n-TP2SS** and to practically no changes for **n-TP2SeS** volume. In the gas phase, the adiabatic energy of the triplet excited states enlarges as the atomic number of the heteroatom does, varying from 0.87 to 1.07 eV. CH_2Cl_2 solvent diminishes this energy gap for all the sapphyrins and, as a consequence, only **n-TP2SS** and **n-TP2SeS** could be adequate to generate singlet molecular oxygen, $^1O_2$ in this environment.

Acknowledgments The authors thank MEC (SPAIN, PCI2005-A7-0304), FONDECYT No 1060203, 1090700 and No 7080007 (CONICYT/CHILE) for financial support. GIC-J thanks to DICYT/USACH Apoyo Complementario for computational time provided.

References

1. Dolphin D (1994) Can J Chem 72:1005
2. Wang Z, Lecane PS, Thiemann P, Fan Q, Cortez C, Ma X, Tonev D, Miles D, Naumovski L, Miller RA, Magda D, Cho DG, Sessler

JL, Pike BL, Yeligar SM, Karaman MW, Hacia GJ (2007) Mol Cancer 6:9
3. Sessler JL, Davis JM (2001) Acc Chem Res 34:989
4. Sessler JL, Seidel D (2003) Angew Chem Int Ed 42:5134
5. Sessler JL, Tvemoes NA, Davis J, Anzenbacher P, Jursikova K Jr, Sato W, Seidel D, Lynch V, Black CB, Try A, Andrioletti B, Hemmi G, Mody TD, Magda DJ, Kral V (1999) Pure Appl Chem 71:2009
6. Boul PJ, Cho DG, Rahman GMA, Marquez M, Ou Z, Kadish KM, Guldi DM, Sessler JL (2007) J Am Chem Soc 129:5683
7. Steiner E, Fowler PW (2004) Org Biomol Chem 2:34
8. Sessler JL, Cho DG, Stepiens M, Lynch V, Waluk J, Yoon ZS, Kim D (2006) J Am Chem Soc 128:12640
9. Rezler EM, Seenisamy J, Bashyam S, Kim MY, White E, Wilson WD, Hurley LH (2005) J Am Chem Soc 127:9439
10. Panda PK, Kang YJ, Lee CH (2005) Angew Chem Int Ed 44:4053
11. Misra R, Chandrashekar TK (2008) Acc Chem Res 41:265
12. Pushpan SK, Chandrashekar TK (2002) Pure Appl Chem 74:2045
13. Chmielewski PJ, Latos-Grazynski L, Rachlewicz K (1995) Chem Eur J 1:68
14. Narayanan SJ, Sridevi B, Chandrashekar TK, Vij A, Roy R (1998) Angew Chem Int Ed 37:3394
15. Pushpan SK, Narayanan SJ, Srinivasan A, Mahajan S, Chandrashekar TK, Roy R (1998) Tetrahedron Lett 39:9249
16. Rachlewicz K, Sprutta N, Chmielewski PJ, Latos-Grazynski L (1998) J Chem Soc Perkin Trans 2:969
17. Brückner C, Sternberg ED, Boyle RW, Dolphin D (1997) Chem Commun 1689
18. Szterenberg L, Latos-Grazynski L (1999) J Phys Chem A 103:3302
19. Szterenberg L, Latos-Grazynski L (1999) J Mol Struct (Theochem) 490:33
20. Cárdenas-Jirón GI, Venegas C, López R, Menéndez MI (2008) J Phys Chem A 112:8100
21. Rachlewicz K, Sprutta N, Latos-Grazynski L, Chmielewski PJ, Szterenberg L (1998) J Chem Soc Perkin Trans 2:959
22. Petit L, Quartarolo AD, Adamo C, Russo N (2006) J Phys Chem B 110:2398
23. Quartarolo AD, Russo N, Sicilia E, Lelj F (2007) J Chem Theory Comput 3:860
24. Sundholm D (2000) Phys Chem Chem Phys 2:2275
25. Shimizu Y, Shen Z, Okujima T, Uno H, Ono N (2004) Chem Commun 374
26. Baker JD, Zerner MC (1990) Chem Phys Lett 175:192
27. Baraldi I, Carnevali A, Ponterini G, Vanossi D (1995) J Mol Struct (Theochem) 333:121
28. Bauernschmitt R, Ahlrichs R (1996) Chem Phys Lett 256:454
29. Foresman JB, Head-Gordon M, Pople JA, Frisch MJ (1992) J Phys Chem 96:135
30. Nagashima U, Takada T, Ohno K (1986) J Chem Phys 85:4524
31. Nooijen M, Barlett RJ (1997) J Chem Phys 106:6449
32. Parusel ABJ, Ghosh A (2000) J Phys Chem A 104:2504
33. Parusel ABJ, Grimme S (2001) J Phorphyrins Phthalocyanines 5:225
34. Yamamoto Y, Noro T, Ohno K (1992) Int J Quantum Chem 42:1563
35. Baerends EJ, Ricciardi G, Rosa A, van Gisbergen SJA (2002) Coord Chem Rev 230:5
36. Kitao O, Ushiyama H, Miura N (1999) J Chem Phys 110:2936
37. Merchán M, Ortí E, Roos BO (1994) Chem Phys Lett 226:27
38. Serrano-Andrés L, Merchán M, Rubio M, Roos BO (1998) Chem Phys Lett 295:195
39. Roos BO, Fülscher MP, Fülscher MP, Malmqvist PA, Merchán M, Serrano-Andrés L (1995) In: Langhoff SR (ed) Quantum mechanical electronic structure calculations with chemical accuracy. Kluwer, Dordrecht, p 357 357
40. Grimme S, Waletzke M (1999) J Chem Phys 111:5645
41. van Gisbergen SJA, Rosa A, Ricciardi G, Baerends EJ (1999) J Chem Phys 111:2499
42. Gwaltney SR, Barlett RJ (1998) J Chem Phys 108:6790
43. Furche F, Ahlrich R (2002) J Chem Phys 117:7433
44. Stratmann RE, Scuseria GE, Frisch MJ (1998) J Chem Phys 109:8218
45. Gaussian 03, Revision E.01, Frisch, MJ, Trucks GW; Schlegel HB, Scuseria GE, Robb MA, Cheeseman JR, Montgomery JA Jr, Vreven T, Kudin KN, Burant JC, Millam JM, Iyengar SS, Tomasi J, Barone V, Mennucci B, Cossi M, Scalmani G, Rega N, Petersson GA, Nakatsuji H, Hada M, Ehara M, Toyota K, Fukuda R, Hasegawa J, Ishida M, Nakajima T, Honda Y, Kitao O, Nakai H, Klene M, Li X, Knox JE, Hratchian HP, Cross JB, Bakken V, Adamo C, Jaramillo J, Gomperts R, Stratmann RE, Yazyev O, Austin AJ, Cammi R, Pomelli C, Ochterski JW, Ayala PY, Morokuma K, Voth GA, Salvador P, Dannenberg JJ, Zakrzewski VG, Dapprich S, Daniels AD, Strain MC, Farkas O, Malick DK, Rabuck AD, Raghavachari K, Foresman JB, Ortiz JV, Cui Q, Baboul AG, Clifford S, Cioslowski J, Stefanov BB, Liu G, Liashenko A, Piskorz P, Komaromi I, Martin RL, Fox DJ, Keith T, Al-Laham MA, Peng CY, Nanayakkara A, Challacombe M, Gill PMW, Johnson B, Chen W, Wong MW, Gonzalez C, Pople JA Gaussian, Inc., Wallingford CT, 2004
46. Becke AD (1998) Phys Rev A 38:3098
47. Becke AD (1993) J Chem Phys 98:5648
48. Lee C, Yang W, Parr RG (1988) Phys Rev B 37:785
49. Hay PJ, Wadt WR (1985) J Chem Phys 82:299
50. Hehre WJ, Radom L, Radom L, Pople JA, Schleyer PvR (1986) Ab initio molecular orbital theory. Wiley, New York
51. Jaguar 5.5, Schrodinger Inc.: Portland, OR, 2004
52. Liu X-J, Pan Q-J, Meng J, Feng J-K (2006) J Mol Struct (Theochem) 765:61
53. Petit L, Adamo C, Russo N (2005) J Phys Chem B 109:12214
54. Adamo C, Barone V (1999) J Chem Phys 110:6158
55. Ernzerhof M, Scuseria GE (1999) J Chem Phys 110:5029
56. Zhao Y, Truhlar DG (2004) J Phys Chem A 108:6908
57. Zhao Y, Truhlar DG (2005) J Chem Theory Comput 1:415
58. Staroverov VN, Scuseria GE, Tao J, Perdew JP (2003) J Chem Phys 119:12129
59. Zhao Y, Truhlar DG (2007) J Chem Theory Comput 3:289
60. Barone V, Cossi M (1998) J Phys Chem A 102:1995
61. Tomasi J, Mennucci B, Cammi R (2005) Chem Rev 105:2999
62. Tomasi J, Persico M (1994) Chem Rev 94:2027
63. Cossi M, Barone V (2001) J Chem Phys 115:4708
64. Improta R, Barone V, Santoro F (2007) Angew Chem Int Ed 46:405
65. Santoro F, Barone V, Gustavsson T, Improta R (2006) J Am Chem Soc 128:16312
66. Scalmani G, Frisch MJ, Mennucci B, Tomasi J, Cammi R, Barone V (2005) J Chem Phys 124:94107
67. Reed AE, Curtiss LA, Weinhold F (1988) Chem Rev 88:899
68. Zhao Y, Schultz NE, Truhlar DG (2005) J Chem Phys 123:161103
69. Zhao Y, Schultz NE, Truhlar DG (2006) J Chem Theory Comput 2:364
70. Zhao Y, Truhlar DG (2008) Acc Chem Res 41:157
71. Gouterman M (1959) J Chem Phys 30:1139
72. Gouterman M (1961) J Mol Spectrosc 6:138
73. Gouterman M (1965) J Mol Spectrosc 16:415
74. Gouterman M, Wagniere GH, Snyder LC (1963) J Mol Spectrosc 11:108
75. Gensch T, Viappiani C, Braslavsky SE (1999) J Am Chem Soc 121:10573

76. Wang Z, Lecane PS, Thiemann P, Fan Q, Cortez C, Ma X, Tonev D, Miles D, Naumovski L, Miller RA, Magda D, Cho DG, Sessler JL, Pike BL, Yeligar SM, Karaman MW, Hacia JG (2007) Mol Cancer 6:1
77. Cho DG, Plitt P, Kim SK, Lynch V, Hong SJ, Lee CH, Sessler JL (2008) J Am Chem Soc 130:10502
78. Zhang P, Steelant W, Kumar M, Scholfield M (2007) J Am Chem Soc 129:4526